Mercury in the global troposphere: a three-dimensional model study

T. Bergan, L. Gallardo*, H. Rodhe

Department of Meteorology, Stockholm University, S-106 91 Stockholm, Sweden

Abstract

The global distributions of elemental mercury (Hg^0) and divalent mercury compounds (HgII) were estimated with a climatological transport model (MOGUNTIA). Natural and man-made sources, including re-emission of previously deposited mercury (of man-made origin), oxidation of Hg^0 to HgII and wet and dry deposition of HgII were explicitly treated. Comparisons with observations of Hg^0 in surface air, HgII in precipitation and trends in mercury deposited in lake sediments and peat bogs show a reasonable agreement if the oxidation rate of Hg^0 was chosen to be 1.0/yr. An oxidation time scale outside the range 0.5–1.5 yr is difficult to reconcile with observations. A recently measured large decrease in the concentrations of Hg^0 over the Atlantic is difficult to explain only by a decrease in man-made emissions in Europe and North America. This latter difficulty indicates either that the man-made emissions have been underestimated or that there are large temporal variations in natural emissions (or re-emissions). We conclude that direct global man-made mercury emissions are likely to be at least 30% as large as the natural emissions, implying that the deposition rate, averaged over the globe, has increased by at least 50% since pre-industrial times. To the extent that re-emission of previously deposited mercury of man-made origin is important, the average deposition rate may well have tripled. In and around the most industrial regions (Europe, North America, Southeastern China) the deposition rate has increased by a factor 2–10 during the past two hundred years. © 1999 Elsevier Science Ltd. All rights reserved.

Keywords: Mercury cycle; global transport model; inorganic mercury; deposition

1. Introduction

Mercury is a volatile element for which transport through the atmosphere plays an important role in its global biogeochemical cycle (e.g. Nriagu, 1979; Fitzgerald, 1986). The fact that elevated – possibly hazardous – levels of mercury have been measured in organisms and in their environment even far away from pollution sources, makes it particularly important to understand the sources and sinks of atmospheric mercury and its distribution throughout the global atmosphere (Lindqvist et al., 1991). Previous studies of the global mercury cycle have been limited to considering global budgets with no explicit consideration of geographical distributions (e.g. Fitzgerald, 1986; Lindqvist et al., 1991; Mason et al., 1994; Hudson et al., 1995). Recently, attempts have been made to formulate quantitative transport models

*Present address: Depto. de Descontaminacion, Planes Y Normas, Comision Nacional del Medio Ambiente (CONAMA), Obispo Donoso 6, Providencia, Santiago, Chile.

covering parts of Europe (Petersen et al., 1995; Galperin et al., 1996) and North America (Shannon and Voldner, 1995).

We believe that the understanding of the various processes in the mercury cycle has now reached a stage where it is meaningful to simulate the global distribution of mercury compounds using a simple chemical tracer transport model. High-quality observational data sets are becoming available from different parts of the globe (e.g. Iverfeldt, 1991; Fitzgerald et al., 1991; Slemr and Langer, 1992; Schroeder, 1994; Slemr, 1996), enabling some degree of testing of such simulations.

In this study we employ a climatological transport model (MOGUNTIA), developed at Max-Planck-Institute for Chemistry in Mainz, Germany (Zimmermann, 1987), to simulate the global distribution of elemental mercury (Hg^0) and divalent mercury compounds (HgII). The main purpose is to see whether present estimates of sources, sinks and atmospheric transformation processes are consistent with observed concentrations of mercury in air, in precipitation and in sediment records. Particularly, we want to estimate the man-made impact on mercury levels in different parts of the world.

2. Model description

2.1. The model

A three-dimensional (3-D) global tracer transport model (MOGUNTIA) has been used to simulate the tropospheric distribution of mercury. The horizontal resolution is $10°$ latitude by $10°$ longitude and there are 10 isobaric levels up to 100 hPa. The transport is based on advection by monthly averaged observed winds and parameterized eddy diffusion (Zimmermann, 1987). Transport in deep cumulus convection is implemented as a stochastic process (Feichter and Crutzen, 1990). A detailed description of the transport representation in MOGUNTIA can be found in Zimmermann et al. (1989) and Langner and Rodhe (1991).

Two mercury reservoirs have been considered in this study: gaseous elementary mercury (Hg^0) and divalent mercury (HgII). No distinction is made between aqueous, gaseous and particulate HgII. Fig. 1 shows the processes, in addition to transport and mixing, included in our model.

2.2. Emissions

Mercury is emitted into the atmosphere from a variety of natural and man-made sources. The former include degassing from soils and oceans and volcanic emissions (Lindqvist et al., 1991), the latter combustion of fossil
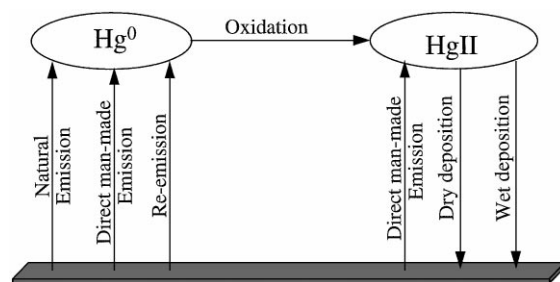

Fig. 1. Schematic illustration of the forms and fluxes of mercury used in the model.

fuels, waste incineration, metal industry, gold extraction, etc. (Nriagu and Pacyna, 1988; Porcella et al., 1997). Large uncertainties are associated with the present estimates of mercury emissions, both in terms of the strength and geographical distribution of the sources. The largest part of the natural emission from land and sea is believed to take place in the form of elemental mercury (Lindqvist et al., 1991). Man-made emissions contain variable fractions of Hg^0 and both gaseous and particulate HgII (Lindqvist et al., 1991).

Estimates of the source strength of man-made emissions vary between about one and six thousand ton Hg per year (Lindqvist et al., 1991; Nriagu and Pacyna, 1988). A detailed compilation of man-made emissions has recently been completed by Pacyna (1998) in the framework of the Global Emission Inventory Activity (GEIA) of IGBP/IGAC. This inventory provides annual global emissions of total mercury on a 1 by $1°$ grid. Fig. 2 shows this GEIA inventory indicating emissions in tons of mercury per gridbox per year. Emissions from waste incineration outside North America was not included in the model because of the sparsity of such data. This may have led to an underestimate of the global man-made emission by about 20% (J.M. Pacyna, personal communication, 1998). Based on Axenfeldt et al. (1991) and Pacyna and Münch (1991) we further assume that 60% of the man-made emissions occur as Hg^0, the rest being the oxidized form, HgII.

Areas affected by deposition originating from previous man-made emissions are assumed to re-emit elemental mercury in proportion to the locally accumulated deposition. The geographical distribution of this re-emission is assumed to be identical with the pattern of total (wet plus dry) deposition resulting from today's man-made emission according to our model calculation. The magnitude of the re-emission has been scaled to match the emissions from soil and vegetation measured in Tennessee, USA by Lindberg et al. (1998). We used a maximum re-emission rate of 150 g/km²/yr (20 ng/m²/h) corresponding to a total global re-emission flux of 2000 ton/yr. Re-emission of previously deposited mercury originating
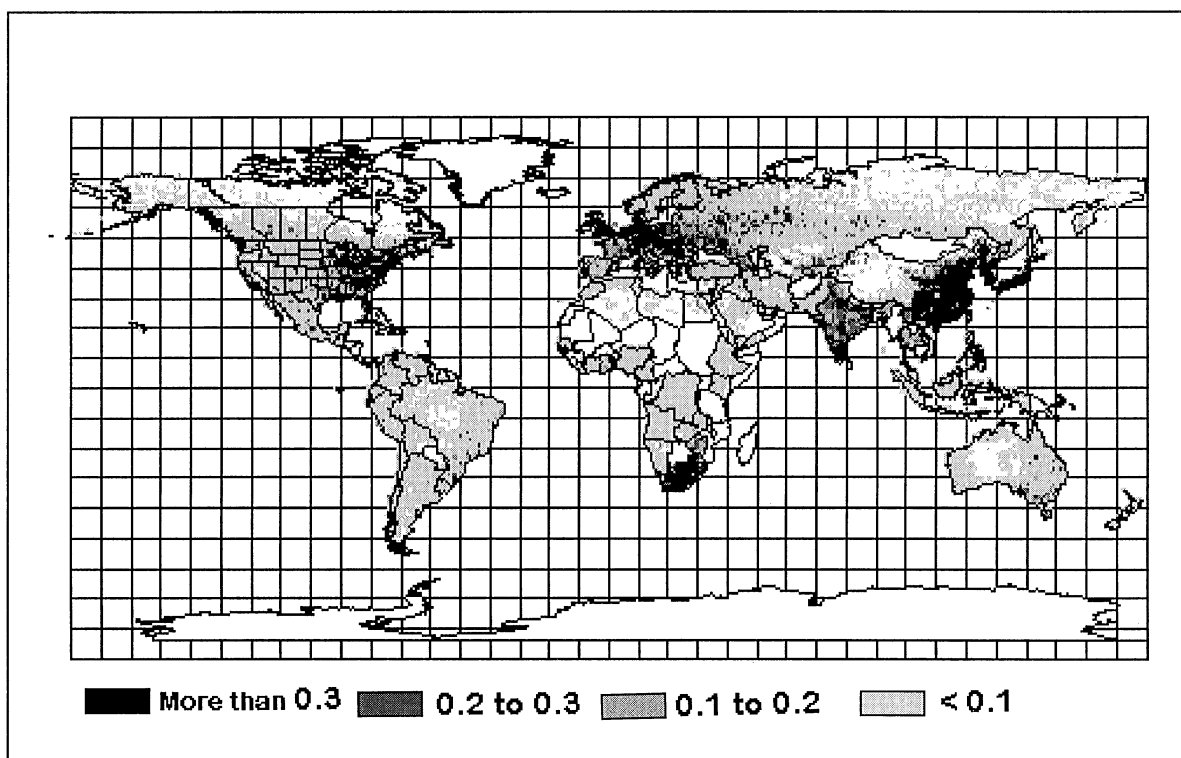
Fig. 2. The man-made mercury emission field used in the model. Adopted from the GEIA inventory of IGBP/IGAC (Pacyna, 1998). Unit: ton Hg/yr per grid box ($1° \times 1°$).

from natural emissions is assumed to be included in the category "natural emissions".

For natural mercury emissions we distinguish between two types of land areas, namely Hg-rich and Hg-poor soils according to Jonasson and Boyle (1971). In the former land type we assume an emission rate ten times larger than in the latter (Lindqvist et al., 1991). The land emission is suppressed in areas covered by ice or snow. The resulting emission field is scaled to yield a global terrestrial emission of 500 ton Hg/yr (Lindqvist et al., 1991; Varekamp and Busek, 1986), all of which assumed to be in the form of Hg^0.

The rate of emission from the oceans is assumed to vary with latitude with the highest values at low latitudes according to observations (Kim and Fitzgerald, 1986; Mason et al., 1994). From thse data we estimate a global emission of 1400 ton Hg^0/yr from the oceans. This figure is the lower end of the range suggested by Lindqvist et al. (1991) and at the upper end of the range suggested by Ryaboshapko and Korolev (1997).

2.3. Chemical transformations

Considerable knowledge has been acquired in the past years regarding the chemistry of mercury transforma-

tions in the atmosphere (Pleijel and Munthe, 1995 and references therein). However, at this early stage we have chosen not to include a detailed chemical scheme. Instead we describe the net transformation of Hg^0 into HgII as a constant oxidation rate. We assume that at every time step, in every grid-box a constant fraction of the Hg^0 is converted to HgII, the constant being the inverse of the turn-over time (τ_{Hg^0}) of Hg^0 in the atmosphere. The turn-over time of Hg^0 has been estimated to be about one year, ranging from 0.3 to 2 yr (Slemr et al., 1985; Lindqvist and Rodhe, 1985; Mason et al., 1994). In our reference case we use a value of 1.0 year.

2.4. Deposition

Deposition processes are believed to affect mainly the HgII reservoir, although some measurements during recent years indicate that dry deposition of Hg^0 may occur, at least locally when the surface air concentration of Hg^0 is high (Lindberg et al., 1992; Xiao et al., 1991).

HgII, in both gaseous and condensed phases, is likely to be readily scavenged by precipitation (Lindqvist et al., 1991 and references therein). Also, a substantial dry deposition flux is likely to take place, especially for the gaseous HgII (Lindberg et al., 1991). Lacking detailed

information about the various forms in which HgII occurs and given the simplicity of our Hg-model, we consider only the deposition of HgII, and we do that in a similar way as the deposition of aerosol sulfate was treated in the global sulfur model by Langner and Rodhe (1991). The deposition velocity of HgII at the surface is assumed to be 0.3 cm/s during day-time and we reduce it by a factor of 2 at night according to estimates by Lindqvist and Rodhe (1985). These values take into account the possibility that a certain fraction of HgII occurs in a soluble gaseous form. The wet removal of HgII is controlled mainly by in-cloud scavenging, yielding a globally averaged time scale of about 2 weeks in our model.

3. Results

3.1. Reference case

The model was first run with the emission scenario specified in Table 1 (the reference case).

3.1.1. Concentrations

The calculated annual mean surface distribution of Hg^0 is shown in Fig. 3. The contribution from the three main man-made emission regions (North America, Europe and Southeastern China) can be clearly distinguished. Since the man-made sources are mainly located in the Northern Hemisphere (NH), the calculated concentrations are lower and more homogeneously distributed in the Southern Hemisphere (SH).

Table 2 summarizes surface observations of Hg^0 made at several sites and the corresponding values calculated by the model. The calculated concentrations agree quite well (within 20%) at most sites.

It should be pointed out that the general magnitude of the simulated concentration of Hg^0 is determined by the balance between the rate of emission and the rate of oxidation. These have to be chosen so that the average concentration level is reasonable. The important question is whether the spatial pattern of the simulated Hg^0 resembles the observed one.

Fig. 4 shows observations of gaseous mercury made over the Atlantic ocean in 1990 and 1994 (Slemr and Langer, 1992; Slemr, 1996). A substantial decrease in the concentration seems to have occurred between 1990 and 1994 at all latitudes north of 35°S. The simulated profile, which is based on man-made emissions in 1990, is also shown in the figure. The model fits reasonably well with the observations in the Atlantic ocean between 30°S and 15°N, but it overestimates the concentrations south of 30°S and it underestimates the concentrations north of 15°N. Overall, the simulated interhemispheric gradient is somewhat too small, especially compared to the 1990

Table 1
Global mercury emissions adopted in the reference case Unit: ton Hg/yr

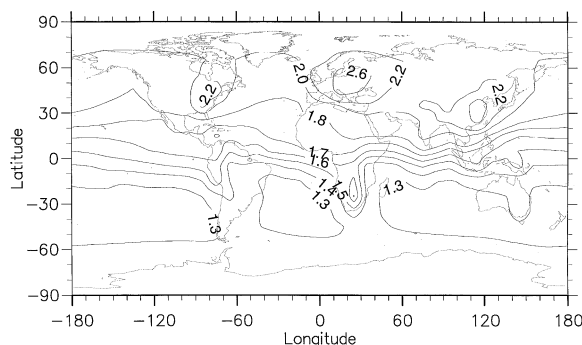| Emission type	Hg^0	HgII	Total
Direct man-made	1300	850	2150
Re-emissions	2000	0	2000
Natural land	500	0	500
Natural sea	1400	0	1400
Total	5200	850	6050

Fig. 3. Global distribution of the annual average concentration of Hg^0 at the lowest model level (250 m) in the reference simulation. Unit: ng Hg/m³.

observations, which is closest to the reference year in the simulation.

This difference might be due to one or several of the following reasons:

(i) inadequacies in the present model, like the latitudinal distribution of sources and oxidation rates,

(ii) the measurements over the Atlantic north of 20°N may have been influenced by episodes of transport from the European continent and may therefore not be representative for long-term average conditions which our model simulate,

(iii) the turn-over time of Hg^0 may be shorter than we have assumed implying that the interhemispheric difference in emissions (higher emissions in the northern hemisphere) would give rise to a larger interhemispheric difference in atmospheric concentration. If this were true, one would also have to assume that the total emissions were higher than those given in Table 1 in order to bring the simulated average concentrations of Hg^0 up to observed levels (cf. Section 3.2).

At the present time it is hardly possible to resolve this issue. Better estimates of the emissions, natural as well as man-made, are clearly required. The only independent

Table 2
Surface concentrations of Hg^0. Unit: ng Hg/m^3

Site	Period of observation	Observation (range or STD)	Model	Reference
Scandinavia				
Øverbygd 69N, 19E	1985–1989	2.6 (1–8)	2.3	Iverfeldt (1991)
Vindeln 64N, 20E	1985–1989	2.5 (1–6)	2.4	Iverfeldt (1991)
Rörvik 57N, 14E	1990–1992	2.7 (1.0)	2.6	Iverfeldt et al. (1995)
Germany				
Wank summit	1990	3.0 (1.0)	2.7	Slemr (1996)
S. Germany	1991	2.8 (0.6)		
	1994	2.3 (0.4)		
Russia				
Baikal Sea	June 1992	1.4 (0.4)	2.1	Meuleman et al. (1995)
54N, 107E	March 1993	2.9 (1.6)		
Canada				
Alert 82N, 62W	August 1992	1.7 (0.5)	2.0	Schroeder et al. (1995)
S. Ontario 44N, 74W	March, April 1990	2.9	2.3	Schroeder (1994)
USA				
N. New York 45N, 73W	1993	1.9 (1.2–4.2)	2.3	Burke et al. (1995)
N. Wisconsin 47N, 89W	1992–1994	1.7 (0.4)	2.1	Lamborg et al. (1995)
C. Wisconsin 46N, 89W	1988–1989	1.6 (0.4)	2.1	Fitzgerald et al. (1991)
Tennessee 35N, 84W	1993–1995	2.2 (0.6)	2.0	Lindberg and Stratton (1998)
Florida	1992–1994	1.6 (0.8)	1.8	Gill et al. (1995)
Florida	1993 (Apr, Sept)	1.8	1.8	Dvonch et al. (1995)
Atlantic Ocean				
7N–54N	Oct/Nov, 1990	2.2 (0.4)	1.6–2.3	Slemr and Langer
48S–7N		1.5 (0.3)	1.2–1.6	(1992)
	Oct/Nov, 1994	1.8 (0.4)		Slemr (1996)
		1.2 (0.2)		

estimate (in the sense that it is not based on estimated sink strengths) of the turn-over time of Hg^0 is that of Slemr et al. (1985) who utilized Junge's (1974) empirical relation between turn-over time of a trace gas and the variability of its concentrations. They estimated that the turn-over time should be about 1 yr, but the uncertainty range is so large that values in the range 0.5–2 yr could not be excluded. The sensitivity of our results to uncertainties in the turn-over time of Hg^0 is discussed in Section 3.2.

3.1.2. Deposition fluxes

The calculated annual HgII wet deposition pattern (Fig. 5) shows maximum deposition over eastern North America, Europe and Southeastern China, in accordance with the prescribed emission pattern. In remote areas most of the HgII originates from the relatively slow transformation of Hg^0. Hg^0 in turn is rather homogene-ously mixed throughout the troposphere due to its relatively long turn-over time (cf. Fig. 2). Therefore, outside the main man-made source regions, the wet deposition of HgII is more homogeneously distributed and it follows largely the distribution of precipitation amounts.

The model dry deposition flux (not shown here) constitutes less than 25% of the total deposition (outside arid regions) and globally it accounts for less than 15% of the total deposition. However, there is at present no means of testing the dry deposition estimates separately.

The sparsity of long-term observations, made on a regular and world-wide basis, makes it difficult to check the calculated wet deposition fluxes. Calculated and observed wet deposition fluxes at several sites are shown in Table 3. The model reproduces the observations rather well, except in Wisconsin, USA and Northern Scandinavia where it overestimates the wet deposition flux. This overestimation near large pollution sources could be
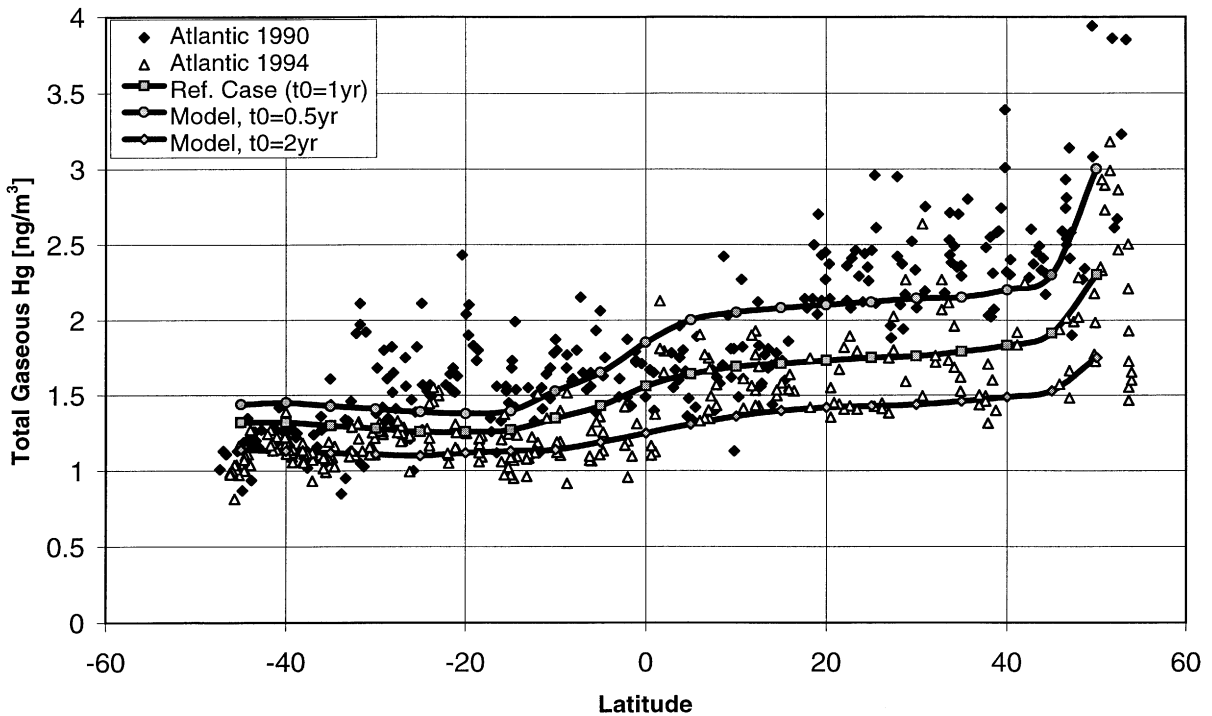
Fig. 4. Distribution of total gaseous mercury over the Atlantic ocean in 1990 (Slemr and Langer, 1992) and 1994 (Slemr, 1996). Three different model simulations are included: the uppermost curve corresponding to a turn-over time of Hg⁰ of 0.5 yr, the middle corresponding to the reference case (1 yr) and the lowest corresponding to a turn-over time of 2 yr.
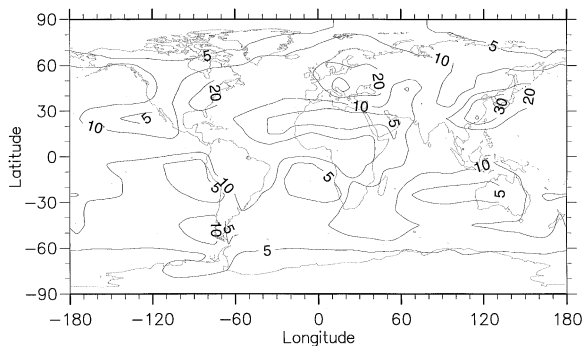

Fig. 5. Global distribution of the annual wet deposition flux of mercury as simulated by the model in the reference case. Unit: g Hg/km^2/yr.

partly due to the inability of a coarse resolution model like MOGUNTIA to treat sharp gradients. Another important factor that affects the testing of wet deposition is the difference between the monthly mean model-precipitation and the amount of precipitation

measured during the period of observation. Again, the sparsity of observations, particularly in remote areas, makes it difficult to draw any definite conclusions.

The turn-over time of HgII depends on the efficiency of the removal processes. In our model the global turn-over time of the HgII, emitted from pollution sources, is about 4 days. If the HgII formed from Hg⁰ is included, the turn-over time is substantially longer (since much of this fraction is formed away from the surface where removal processes are less efficient), C.f. Section 2.4.

3.1.3. Amplification factor

Another check of the model performance can be made through a comparison of the calculated and the observed "Amplification Factor" (AF). This factor is defined as the ratio between the total deposition at the present time and the total deposition during pre-industrial times. In the model this factor is calculated by dividing the total deposition field obtained in a simulation with all emissions included and the corresponding field obtained suppressing the man-made emissions (including re-emissions). The observed AF values are derived from observed profiles of mercury in lake sediments and peat bogs. Such profiles, most of them obtained in Europe and

Table 3
Annual HgII wet deposition. Unit: g Hg/km^2/yr

Site	Observation (Range)	Model	Reference
Scandinavia			
Northern Norway	3–5	12–15	Iverfeldt (1991)
Northern Sweden	10	12–16	Iverfeldt (1991)
SW Sweden			
1985–1989	27	20–25	Iverfeldt (1991)
1990–1992	10		Iverfeldt et al. (1995)
USA			
N New York State 1993	10	20–25	Burke et al. (1995)
NE Minnesota 1988–1989	15 (6–20)	13	Glass et al. (1991)
Wisconsin	9 (5–13)	25	Fitzgerald et al. (1994)
Florida, 1992–1993	15–23	15–18	Guentzel et al. (1995)
Japan			
Kobe	40	30–35	Lindberg et al. (1992)
Oceanic			
NW Atlantic	11	15–20	Fitzgerald (1989)
Tropical Pacific	3	8–11	Fitzgerald et al. (1983)
NE Pacific	10	8–14	Fitzgerald (1989)
Enewetak (11N, 165E)	4.2	10	Fitzgerald (1989)
Samoa (13S, 170W)	7.0	10	Fitzgerald (1989)
Tasman Sea (35S, 170E)	3.8	8	Fitzgerald (1989)

North America, show a very conspicuous increase in concentration during the past decades or centuries, presumably due to man-made emissions.

Fig. 6 shows the calculated amplification factor. The largest AF values are found over eastern North America, Europe and Southeastern China, in accordance with the prescribed emission pattern. A narrow maximum of AF is also found in Southern Africa in connection with a large point source (smelter). Notice that the increase in mercury deposition is not only confined to the regions where man-made emissions occur. According to our calculations, a large increase (AF > 3) in total deposition has taken place also over remote oceanic and continental areas, in most of the NH. In the remote parts of the SH the amplification factor varies between 2 and 3. The relatively high value of the AF even in remote areas is due to the fact that a substantial fraction of the man-made emissions occur in the form of Hg^0, which has a long turn-over time and a relatively uniform global distribution.

Only a few estimates of AF based on measurements are available in the literature. Table 4 shows these estimates and the corresponding model estimates. The agreement between the estimates is encouraging. However, we caution the reader from drawing far-reaching conclusions from this agreement. The representativity and the precision of the sediment data have not been well established.
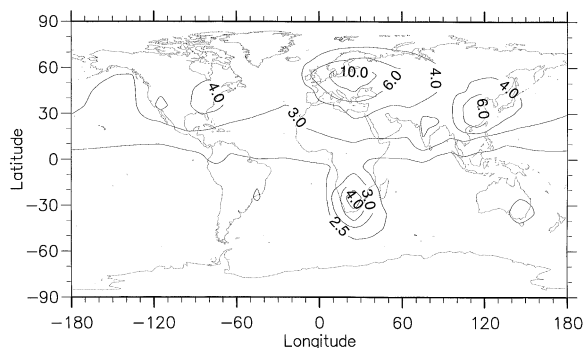

Fig. 6. Global distribution of the "Amplification Factor", defined as the ratio between the present and pre-industrial mercury deposition, in the reference case.

3.2. Sensitivity tests

In order to test how sensitive the model results are to changes in the oxidation rate of Hg^0, we have run the model also with an oxidation time scale of 2 and 0.5 yr. If such changes are introduced without corresponding modifications of emission rates, the average concentration of Hg^0 increases and decreases with a factor of two in the first and second case, respectively. To avoid such

Table 4
Estimates of the amplification factor (AF) in total mercury deposition as derived from sediment cores and model calculations

Site	Observation	Model	Reference
Scandinavia			
Northern Sweden (lakes)	< 2	5	Johansson (1985)
Northern Finland (lakes)	3 (1–6)	5	Verta et al. (1990)
Southern Sweden (lakes)	5	10–12	Johansson (1985)
Southern Finland (lakes)	6 (1–16)	8	Verta et al. (1990)
North America			
USA (lakes)	3.4	3–5	Swain et al. (1992)
USA (bogs)	> 2.5		Benoit et al. (1994)
Canada (lakes)	1.2–7		Lockhart et al. (1995)

unrealistic changes in the concentration of Hg^0, the total emission of Hg^0 had to be halved and doubled, respectively. These changes are still within the uncertainty ranges of the natural emissions reported in the literature (cf. Section 2.2). In the simulation with $\tau_0 = 0.5$ yr the latitudinal gradient is more pronounced improving the agreement between simulated and observed latitudinal gradient (cf. Fig. 4). However, this scenario implies a large increase in the sources and sinks of HgII, resulting in a substantial overestimate in the wet deposition rates (cf. Table 3). The curve in Fig. 4 corresponding to this case is based on a Hg^0 emission scenario including 2150 ton/yr from direct man-made emission, 5000 ton from re-emission, 1050 ton from natural continental emission and 3500 ton from the oceans. If Hg^0 had substantial sinks in addition to the oxidation to HgII, e.g. dry deposition, a faster oxidation rate could possibly still be reasonably consistent with observations. The turn-over time of Hg^0, corresponding to the total sink strength, could then be 0.5–1 yr.

In the simulation with a slower oxidation rate ($\tau_0 = 2$ yr), the latitudinal gradient is weaker than in the reference case (cf. Fig. 4). The lower emission rates of Hg^0 that we have to prescribe in this case lead to a smaller rate of formation and deposition of HgII. The wet deposition of HgII is still in fair agreement with observations, albeit in the lower range, especially in Europe and North America.

In order to test the sensitivity of our results to the assumption of how the man-made emissions are distributed between Hg^0 and HgII, we performed a simulation where the HgII fraction was increased from 40 to 70%. The results (not shown) indicate more pronounced peaks in the mercury deposition in the main source regions. The maximum deposition increased by 40% in Central Europe, 25% in China and 10% in Eastern US. Only minor changes in the deposition occur in remote areas. A comparison of the wet deposition fluxes in this simulation with observations (Table 3) shows a somewhat poorer agreement in the polluted regions compared to the refer-

ence case. This suggests that the HgII fraction in man-made emissions is more likely to be below 50% than above. However, none of our general conclusions would be invalid if the assumption of 40% HgII fraction in the man-made emissions were increased to 50% or decreased to 30%.

A further test was carried out assuming that no emissions occur from the oceans. The same flux as the ocean source in the reference case (1400 ton/yr, cf. Table 1) was instead added to the natural terrestrial source. The latitudinal gradient in Hg^0 turned out to be quite similar to that in the reference case (cf. Fig. 4). No substantial differences occurred in the concentration of Hg^0 and wet-deposition of HgII. Thus we cannot rule out the possibility that the ocean source is substantially smaller than previously believed and that the dominant part of the natural emissions take place on the continents.

The comparatively large values of model-simulated AF over Europe may indicate that we have exaggerated the man made impact on the global mercury cycle by assuming that the predominant part of the measured flux, obtained from Linberg et al. (1998) (cf. Section 2.2), originates from re-emissions with man-made origin. If instead one assumes that this "re-emission" is entirely of natural origin, the modeled AF is reduced by about a factor of two in the reference case. Such an emission scenario, which may be considered as a limiting case giving a lower limit of the AF, is still reasonably consistent with the AF observations shown in Table 4.

3.3. Impact of man-made sources in Europe and North America

Whereas measurements made over the Atlantic ocean in the 1970s and 1980s indicated an upward trend of 1–2%/yr in total gaseous mercury (Slemr and Langer, 1992), more recent data show a decreasing trend in surface concentrations and deposition fluxes of mercury in both polluted and remote areas (Iverfeldt et al., 1995; Benoit et al., 1994; Engstrom and Swain, 1996; Slemr et

al., 1995; Pacyna and Berg, 1996; Slemr, 1996; Slemr and Scheel, 1998). Such decrease might be attributed to a decrease in man-made emissions from large sources in central Europe and Northeastern America. For example, the closing down of large coal-fired power plants in former East Germany is likely to have led to a substantial reduction in the mercury emission in this region (Slemr and Scheel, 1998).

By switching off the direct man-made emissions in these regions in the model simulations we can assess their contribution to the world-wide concentration and the deposition fluxes of mercury. Fig. 7 shows the calculated percentage contribution of man-made emissions in Northeastern America and in Europe to the surface concentrations of Hg^0. These two regions account, according to the GEIA inventory, for about 30% of the global man-made emissions. Due to the long turn-over time of Hg^0, the contribution from these sources is relatively evenly distributed over the world, with a moderate inter-hemispheric gradient and a somewhat stronger impact close to the sources. The geographical pattern of the contribution of the North American and European sources to the total *deposition* of mercury is much more confined to the source areas than that shown in Fig. 7.

The decrease in mercury concentration and depositions during the 1990s reported by Iverfeldt et al. (1995) and Pacyna and Berg (1996) from Scandinavia, Slemr (1996) from Southern Germany and by Benoit et al. (1994) and Engstrom and Swain (1996) from the USA can possibly be quantitatively explained by a decline in the man-made emission in these two regions. However, the decline by 20% in gaseous mercury (mainly Hg^0) measured by Slemr et al. (1995) over the Atlantic (between 1990 and 1994) is difficult to explain by the same argument alone. It would not even suffice if all man-made mercury emissions in Europe and North America dropped to zero during these four years, as in the simulation shown in Fig. 7. The increase in mercury emissions that is likely to have occurred in parts of Asia during recent years, makes it even harder to reconcile our model simulations with the observations by Slemr et al. (1995).

If the measurements by Slemr et al. (1995) are representative for average conditions (as simulated by our model) one is led to the conclusion that *either* the relative magnitude of man-made to natural Hg^0 emissions has been underestimated *or* – more likely – the natural emissions undergo large variations from year to year or from decade to decade. More long-term measurements of Hg^0 and HgII in air and in precipitation are needed before this issue can be resolved.

4. Conclusions

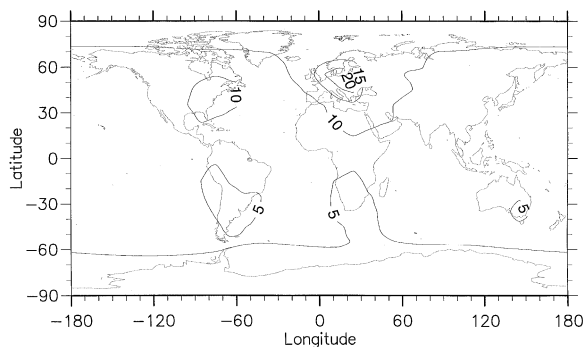We have used a climatological transport model to simulate the distribution of gaseous elemental mercury

Fig. 7. Percentage reduction in surface concentration of Hg^0 in a hypothetical situation where all direct man-made mercury emissions have been eliminated in the eastern part of North America and in Europe.

(Hg^0) and divalent mercury (HgII) in the global troposphere. Estimates of natural and man-made emissions were taken from the literature. Comparisons were made with measurements of Hg^0 in surface air, HgII in precipitation and deposition of total mercury in lake sediments and in peat bogs. Although such data exist only from a very limited part of the globe, there is a rough overall agreement between simulated and observed concentration patterns. This indicates, but does not prove, that the assumptions about emission, transformation and deposition processes are reasonably realistic.

However, recent observations of a large decrease in the concentration of total gaseous mercury (most of it likely to be Hg^0) over the Atlantic during the 1990s (Slemr et al., 1995) are hard to explain with the model using current estimates of sources, transformation and sinks. These data seem to indicate that the relative magnitude of man-made emissions has been underestimated or that large variations occur in the natural part of the mercury cycle.

Bearing this uncertainty in mind, we still believe that the following conclusions are supported by our study.

- The turn-over time of Hg^0 in the global atmosphere is in the range 0.5–1.5 yr.
- The magnitude of the direct man-made mercury emissions into the atmosphere are likely to be at least 30% of the magnitude of the natural emissions, implying that the deposition rate, averaged over the globe, has increased by at least 50% since pre-industrial times. Assuming furthermore that there is a re-emission of previously deposited mercury of man-made origin, this increase may be as large as a factor of three.
- In and around the most industrial regions (Europe, North America, SE China) the deposition rate of mercury is likely to have increased by a factor 2–10 during the past 200 yr.

In order to reduce the uncertainties in the estimates of the global distribution of mercury, it is necessary to obtain more long-term measurements of the concentration of mercury in air and of its fluxes to and from the surface, especially at remote sites in the tropics, subtropics and mid to high latitudes in the Southern Hemisphere.

Acknowledgements

References

Axenfeldt, F., Münch, J., Pacyna, J., 1991. Europäische Testemissionsdatenbasis von Quecksilberkomponenten für Modellrechnungen. Umweltforchungsplan des Bundesministers für Umwelt, Naturschutz und Reaktorsicherheit-Luftreinhaltung-104 02 726.

Benoit, J.M., Fitzgerald, W.F., Damman, A.W., 1994. Historical atmospheric mercury deposition in the midcontinental U.S. as recorded in an ombotrophic peat bog. In: Watras, C., Huckabee, J. (Eds.), Mercury Pollution: Integration and Synthesis, Ch. II.2. Lewis Publishers, Boca Raton, Florida.

Burke, J., Hoyer, M., Keeler, G., Scherbatskoy, T., 1995. Wet deposition of mercury and ambient mercury concentrations at a site in the Lake Champlain basin. Water, Air and Soil Pollution 80, 353–362.

Dvonch, J.T., Vette, A.F., Keeler, G., Evans, G., Stevens, R., 1995. An intensive multi-site pilot study investigating atmospheric mercury in Broward County, Florida. Water, Air and Soil Pollution 80, 169–178.

Engstrom, D.R., Swain, E.B., 1996. Recent declines in atmospheric mercury deposition in the upper Midwest, USA. Abstract from the 4th International Conference on Mercury as a Global Pollutant, 4–8 August 1996, Hamburg, pp. 55.

Feichter, J., Crutzen, P., 1990. Parameterization of vertical tracer transport due to cumulus convection in a global transport model and evaluation with ^{222}Radon measurements. Tellus 42 B, 100–117.

Fitzgerald, W.F., Gill, G.A., Hewitt, A.D., 1983. Trace Metals in Sea Water. In: C.S. Wong et al. (Eds.), Plenum, New York, 1983, pp. 297–315.

Fitzgerald, W.F., 1986. Cycling of mercury between the atmosphere and oceans. The Role of Air-Sea Exchange in Geochemical. NATO Advanced Institute Series, vol. C185, Reidel, Dordrecht, The Netherlands, pp. 363–408.

Fitzgerald, W.F., 1989. Atmospheric and oceanic cycling of mercury. Chemical Oceanography Series, Ch. 57, vol. 10. Riley, J.P., Chester, R. (Eds.), Academic Press, New York, pp. 151–186.

Fizgerald, W.F., Mason, R.P., Vandal, G.M., 1991. Atmospheric cycling and air water exchange of mercury over mid continental lacustrine regions. Water, Air and Soil Pollution 56, 745–767.

Fitzgerald, W.F., Mason, R.P., Vandal, G.M., Dulac, F., 1994. Air-water cycling of mercury in lakes. In: Watras, C., Huckabee, J. (Eds.), Mercury Pollution: Integration and Synthesis. Lewis Publishers, Chelsea, pp. 203–220.

Galperin, M., Sofiev, M., Mantseva, E., 1996. A model of the geochemical transformation of mercury and its long-range atmospheric transport. In: Baeyens, W. et al. (Eds.), Global and Regional Mercury Cycles: Sources, Fluxes and Mass Balances. NATO ASI Series, 2. Environment, vol. 21. Kluwer Academic Publ., Dordrecht, pp. 219–227.

Gill, G.A., Guentzel, J.L., Landing, W.M., Pollman, C.d., 1995. Total gaseous mercury measurements in Florida: the FAMS Project (1992–1994). Water, Air and Soil Pollution 80, 235–244.

Glass, G.E., Sorensen, J.A., Schmidt, K.W., Rapp, G.R., Yap, D., Fraser, D., 1991. Mercury deposition and sources for upper Great Lakes region. Water, Air and Soil Pollution 56, 235–250.

Guentzel, J.L., Landing, W.M., Gill, G.A., Pollman, C.D., 1995. Atmospheric deposition of mercury in Florida: the FAMS Project (1992–1994). Water, Air and Soil Pollution 80, 393–402.

Hudson, R.J.M., Gherini, S.A., Fitzgerald, W.F., Porcella, D.B., 1995. Anthropogenic influence on global mercury cycle: A model-based analysis. Water, Air and Soil Pollution 80, 265–272.

Iverfeldt, Å., 1991. Occurrence and turnover of atmospheric mercury over the Nordic countries. Water, Air and Soil Pollution 56, 251–265.

Iverfeldt, Å., Munthe, J., Brosset, C., Pacyna, J., 1995. Long term changes in concentration and deposition of atmospheric mercury over Scandinavia. Water, Air and Soil Pollution 80, 227–233.

Johansson, K., 1985. Verhandlungen Internationale Vereinigung Limnologie 22, 2359–2363.

Jonasson, I.R., Boyle, R.W., 1971. Geochemistry of mercury. Proceedings of Special Symposium on Mercury in Man's Environment, 15 and 16 February, 1971. Royal Society of Canada, Ottawa, Ontario.

Junge, C.E., 1974. Residence time and variability of tropospheric trace gases. Tellus 26, 477–488.

Kim, J.P., Fitzgerald, W.F., 1986. Sea air partitioning of mercury in the equatorial Pacific Ocean. Science 231, 1131–1133.

Langner, J., Rodhe, H., 1991. A global three-dimensional model of the tropospheric sulfur cycle. Journal of Atmospheric Chemistry 13, 225–263.

Lamborg, C.H., Fitzgerald, W.F., Vandal, G.M., Rolfhus, K.R., 1995. Atmospheric mercury in northern Wisconsin: sources and species. Water, Air and Soil Pollution 80, 189–198.

Lindberg, S.E., Turner, R.R., Meyers, T.P., Tylor, G.E., Schroeder, W.H., 1991. Atmospheric concentration and deposition of Hg to a deciduous forest at Walker Branch Watershed, Tennessee, USA. Water, Air and Soil Pollution 56, 577–594.

Lindberg, S.E., Meyers, T.P., Taylor, G.E., Turner, R.R., Schroeder, W.H., 1992. Atmosphere-surface exchange of mercury in a forest: results of modeling and gradient approaches. Journal Geophysical Research 97, 2519–2528.

Lindberg, S.E., Hanson, P.J., Meyers, T.P., Kim, K.-H., 1998. Air/surface exchange of mercury vapor over forests – the need for a reassessment of continental biogenic emissions. Atmospheric Environment 32, 895–908.

Lindberg, S.E., Stratton, W.J., 1998. Atmospheric mercury speciation: concentrations and behavior of reactive gaseous mercury in ambient air. Environmental Science and Technology 32, 49–57.

Lindqvist, O., Rodhe, H., 1985. Atmospheric mercury – a review. Tellus, 37B, 136–159.

Lindqvist, O., Johansson, K., Aastrup, M., Andersson, A., Bringmark, L., Hovsenius, G., Håkanson, L., Iverfeldt, Å., Meili, M., Timm, B., 1991. Water, Air and Soil Pollution 55, 1–261.

Lockhart, W.L., Wilkinson, P., Billeck, B.N., Hunt, R.V., Wagemann, R., Brunskill, G.J., 1995. Current and historical input of mercury to high latitude lakes in Canada and Hudson Bay. Water, Air and Soil Pollution 80.

Mason, R.P., Fitzgerald, W.F., Morel, F.M.M., 1994. The biogeochemical cycling of elemental mercury: anthropogenic influences. Geochemica et Cosmochemica Acta 58, 3191–3198.

Meuleman, C., Leermakers, M., Henry, E.A., 1995. Mercury speciation in Lake Baikal. Water, Air and Soil Pollution 80, 539–551.

Nriagu, J.O., 1979. The biochemistry of mercury in the environment. The Evolution of Chemistry. Roland Publ. Co., New York.

Nriagu, J.O., Pacyna, J.M., 1988. Quantitative assessment of worldwide contamination of air, water and soil by trace metals. Nature 333, 134–139.

Pacyna, J.M., Münch, J., 1991. Anthropogenic mercury emissions in Europe. Water, Air and Soil Pollution 56, 51–61.

Pacyna, J.M., Berg, Y., 1996. Change of atmospheric mercury levels in Norway. Abstract of the 4th International Conference on Mercury as a Global Pollutant. 4–8 August 1996, Hamburg, pp. 466.

Pacyna, J.M., 1998. Heavy metals. Chapter 7 of the AMAP Assessment Report: Arctic Pollution Issues. The Arctic Monitoring and Assessment Programme, P.O. Box 8100, N-0037 Oslo, Norway.

Petersen, G., Iverfeldt, Å., Munthe, J., 1995. Atmospheric mercury species over Central and Northern Europe. Model calculation and comparison with observation from the Nordic air and precipitation network for 1987 and 1988. Atmospheric Environment 29, 47–67.

Pleijel, K., Munthe, J., 1995. Modeling the atmospheric mercury cycle-Chemistry in fog droplets. Atmospheric Environment 29, 1441–1457.

Porcella, D.B., Ramel, C., Jernelöv, A., 1997. Global mercury pollution and the role of gold mining: an overview. Water, Air and Soil Pollution 97, 205–207.

Ryaboshapko, A.G., Korolev, V.A., 1997. Mercury in the atmosphere: estimates of model parameters. EMEP/MSC-E Report 7/97.

Schroeder, W.H., 1994. Atmospheric mercury measurements at a rural site in southern Ontario, Canada. In: Watras, C., Huckabee, J. (Eds.), Mercury Pollution: Integration and Synthesis. Lewis Publishers, Chelsea, pp. 231–241.

Schroeder, W.H., Ebinghaus, R., Shoeib, M., Timoschenko, K., Barrie, L.A., 1995. Atmospheric mercury measurements in the northern hemisphere from 56 to 82.5°N latitude. Water, Air and Soil Pollution 80, 1227–1236.

Shannon, J.D., Voldner, E.C., 1995. Modeling atmospheric concentrations of mercury and deposition to the Great Lakes. Atmospheric Environment 29, 1649–1661.

Slemr, F., Schuster, G., Seiler, W., 1985. Distribution, speciation and budget of atmospheric mercury. Journal of Atmospheric Chemistry 3, 407–434.

Slemr, F., Langer, E., 1992. Increase in global atmospheric concentrations of mercury inferred from measurements over the Atlantic Ocean. Nature 355, 434–437.

Slemr, F., Junkermann, W., Schmidt, R.W.H., Sladkovic, R., 1995. Indication of change in global and regional trends of atmospheric mercury concentrations. Geophysical Research Letters 22, 2143–2146.

Slemr, F., 1996. Trends in atmospheric mercury concentrations over the Atlantic ocean and the Wank Summit, and the resulting constraints on the budget of atmospheric mercury. In: Baeyens, W., Ebinghaus, R., Vasiliev, O. (Eds.), Global Regional Cycles: Sources, Fluxes and Mass Balance. NATO-ASI-Series. Kluwer Academic Publishers, Dordrecht, The Netherlands, pp. 33–48.

Slemr, F., Scheel, H.E., 1998. Trends in atmospheric mercury concentrations at the summit of the Wank Mountain, Southern Germany. Atmospheric Environment 32, 845–853.

Swain, E.B., Engstrom, D.R., Brigham, M.E., Henning, T.A., Brezonik, P.L., 1992. Increasing rates of atmospheric mercury deposition in midcontinental North America. Science 257, 784–787.

Varekamp, J.C., Busek, P.R., 1986. Global mercury flux from volcanic and geothermal sources. Applied Geochemistry 1, 65–73.

Verta, M., Mannio, J., Iivonen, P., Hirvi, J.-P., Järvinen, O., Pieppoonen, S., 1990. In: Kauppi, P., Kenttämies, K., Anttila, P. (Eds.), Acidification in Finland, Springer, Heidelberg, pp. 833.

Xiao, Z., Munthe, J., Schroeder, E.W., Lindqvist, O., 1991. Vertical fluxes of volatile mercury over forests, soil and lake surfaces in Sweden. Tellus 43B, 267–279.

Zimmermann, P., 1987. MOGUNTIA a handy global tracer model. XVI NATO/CCMS International Technical Meeting on air pollution modeling and application, 6–10 April Lindau, Lake Constance, FRG.

Zimmermann, P., Feichter, L., Rath, H., Crutzen, P., Weiss, W., 1989. A global three-dimensional source receptor model investigation using ^{85}Kr. Atmospheric Environment 23, 25–35.